Journal of Oral Science, Vol. 52, No. 2, 203-211, 2010

Original

A comparative study of microfocus CT and histomorphometry in the evaluation of bone augmentation in rat calvarium

Go Kochi[1)], Shuichi Sato[2,3)], Hajime Ebihara[2)], Jiro Hirano[2)], Yoshinori Arai[4)] and Koichi Ito[2,3)]

[1)]Division of Applied Oral Sciences, Nihon University Graduate School of Dentistry, Tokyo, Japan
[2)]Department of Periodontology, Nihon University School of Dentistry, Tokyo, Japan
[3)]Division of Advanced Dental Treatment, Dental Research Center, Nihon University School of Dentistry, Tokyo, Japan
[4)]Nihon University School of Dentistry, Tokyo, Japan

(Received 15 December 2009 and accepted 25 January 2010)

Abstract: Microfocus computed tomography (micro-CT; R_mCT) is a dynamic noninvasive method for measuring bone regeneration. This study evaluated whether R_mCT was equivalent to histomorphometry in assessing bone augmentation. Two plastic caps of graft material with (experiment) or without hydroxyapatite (HA; control) were placed in the exposed calvaria of rats. Images of bone augmentation within the plastic caps were then taken using R_mCT. Histological sections were cut along the same plane as that used for the micro-CT images. Bone regeneration beyond the skeletal envelope occurred at both the experimental and control sites. Bone volume also increased at both sites. In addition, consistent patterns of bone formation were observed in both R_mCT and histological images. R_mCT analysis enables highly quantitative and qualitative measurement of bone augmentation in living animals. (J Oral Sci 52, 203-211, 2010)

Keywords: micro-CT; bone augmentation; rat calvaria; animal study.

Correspondence to Dr. Shuichi Sato, Department of Periodontology, Nihon University School of Dentistry, 1-8-13 Kanda-Surugadai, Chiyoda-ku, Tokyo 101-8310, Japan
Tel: +81-3-3219-8107
Fax: +81-3-3219-8349
E-mail: sato-su@dent.nihon-u.ac.jp

Introduction

The ability of guided bone augmentation (GBA) to produce bone has been documented in animal experiments and clinical studies (1-4), and a GBA method that uses space-making barrier membranes to promote new bone growth beyond the skeletal envelope has been developed (5-7). Strictly speaking, GBA involves creating new bone by guiding bone cells to an area beyond the original outer or inner skeletal envelope. Autogenous bone is the gold standard for filling materials, but its use is limited due to the possibility of complications (8,9). β-tricalcium phosphate (β-TCP) and hydroxyapatite (HA) have been used in experimental and clinical studies (10,11). Previously, we showed that β-TCP was effective for bone augmentation beyond the skeletal envelope in rabbit (10).

Because continuous observation of the dynamics of bone augmentation in the same animal is difficult, many laboratory animals must be used and sacrificed for such observations. However, a microfocus computed tomography (micro-CT; R_mCT) system can obtain images of anesthetized animals secured to a stage (12). This system produces high-resolution images, is quick, delivers only a low effective dose of radiation, and can produce clear images of bones in small living animals. Min et al. (13) used R_mCT to observe the dynamics of bone augmentation without graft materials in rabbit calvaria. In a previous study (14), we used R_mCT to examine bone augmentation beyond the skeletal envelope in rat calvaria,

with or without HA. The present study evaluated whether R_mCT was equivalent to histomorphometry in assessing bone augmentation beyond the skeletal envelope in rat calvaria.

Materials and Methods

Eight 12-week-old male Wistar rats weighing 2.5-2.8 kg were used. The animals were housed in metal cages at a temperature of 22°C, with a 12/12-h light/day cycle. This study was approved by the Animal Experimentation Committee of Nihon University School of Dentistry, Japan. The animals were anesthetized with an intraperitoneal injection of 0.5 ml of a 1:8 dilution of lidocaine (Xylocaine; Astra Zeneca, Osaka, Japan). The dorsal cranium was shaved and prepared aseptically for surgery. A 20-mm-long incision was made in the scalp along the sagittal suture. In each rat, a circular groove was made on each side of the midline, using a trephine drill with an inner diameter of 5 mm under profuse irrigation with sterile saline. Five small holes were drilled with a number 2 round burr to induce bleeding from the bone marrow space within each circle. The circular groove and 5 holes were created carefully so as not to penetrate the dura (Fig. 1a). A cylindrical plastic cap was pressed into the circular grooves on both sides of the midline, and composite resin landmarks were fixed on the plastic caps. The mid-sagittal suture was not included in the bone defect to ensure that it did not contribute to bone healing and to limit the risk of damaging the superior sagittal sinus. Before placement, the plastic cap was filled with high-porosity hydroxyapatite (HA, porosity 82.5%, pore size 600 – 1,000 μm, weight 8 mg, APACERAM-AX®; Pentax, Tokyo, Japan) for the experimental site or left empty for the control site (Fig. 1b).

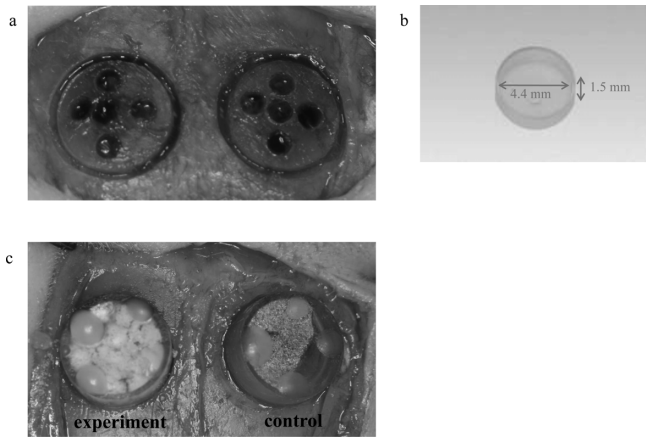

Fig. 1 a) A 5-mm circular groove was made with a trephine, and 5 small holes were drilled with a round burr; b) a plastic cap, and c) plastic caps fixed in the grooves. The experimental group had HA in the plastic cap; the control plastic cap was moistened by breathing.

The R_mCT system (Rigaku, Tokyo, Japan) uses a microfocus X-ray tube with a focal point of 7 μm (L9181S; Hamamatsu Photonics, Hamamatsu, Japan); the X-ray sensor has a 4inch image intensifier. The X-ray source and image intensifier are connected by a basal plate. The I-arm rotates on the vertical plane, and is driven by a direct-drive motor. Each rat was anesthetized with sodium pentobarbital. Under anesthesia, the rat was placed on the object stage. The rat underwent repeated R_mCT from 1 to 12 weeks postoperatively.

The exposure parameters were 90 kV and 88 μA. The images were reconstructed on a personal computer using custom I-VIEW software. The relative CT values of cortical bone and soft tissue were measured using R_mCT. We also measured the bone volume (BV) within the plastic cap using voxel images and BV-measuring software (Kitasenjyu Radist Dental Clinic, I-VIEW Image Center, Tokyo, Japan). The thresholds for HA, newly generated tissue, and mineralized bone from Kochi et al. (14) were employed. Using the BVmeasuring software, the gray values and number of voxels with the corresponding gray value were

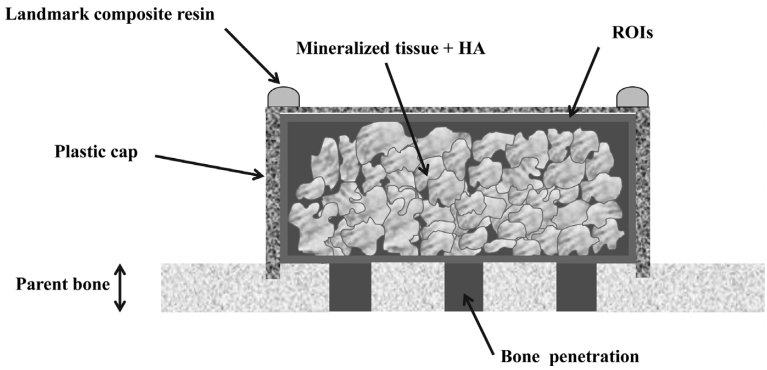

Fig. 2 A schema of the plastic cap and area visualized using R_mCT indicated as ROIs.

calculated in regions of interest (ROIs; Fig. 2). A histogram plotting the X-ray absorption rate on the x-axis against the CT voxel numbers on the y-axis was created for the field of view of the CT imaging area. The histograms of the X-ray absorption rates showed peaks for hard and soft tissues. Then, the threshold was set at the value for the trough between these peaks. The number of voxels for the X-ray absorption rates that exceeded this threshold was counted. Finally, the BV was calculated and the number of voxels was multiplied by the voxel volume. The BV was measured on the first postoperative day in the ROIs and again each week under the same conditions. Then, the increase in BV was calculated by subtracting the BV on day 1 from each subsequent value. The increase in bone was considered to be new bone.

At 12 weeks, ie, after the last micro-CT scan, the rats were euthanized with an overdose of pentobarbital. The calvarial bone with the plastic cap was resected, fixed in 10% neutral buffered formalin, dehydrated, embedded in paraffin, and processed into 4 to 5mm-thick hematoxylin and eosin sections. One sagittal decalcified ground section from the center of the plastic cap was prepared with a microtome. We performed a histological and morphometric assessment of the sections under a light microscope equipped with a morphometric system connected to a personal computer. The histomorphometry data for the central section obtained from each specimen were recorded using a computerized image analysis system. Images taken at ×3 magnification were digitized using a solid-state 35-mm slide scanner and a charge-coupled device (CCD) linear photodiode array interfaced to the computer. Measurements were extracted from the digital images using an interactive image-processing software package.

For each central histological section, we calculated the percentages of areas of newly generated tissue and mineralized bone relative to the area bounded by the plastic cap and parent bone (this last area was designated as 100%). We determined the cross-sectional area of newly generated tissue and mineralized tissue, which was expressed as a percentage of the height and total area of the tissue generated within each space (Fig. 3). Then, a representative histological section was selected and compared with the appropriate CT image, taking care to match specific homologous anatomical features in the bony anatomy.

Statistical analysis

Means and standard deviations were calculated for bone volume, height, and percentages of areas of newly generated tissue and mineralized bone under the plastic caps after 12 weeks. The Wilcoxon signed rank test was used to analyze differences between the experimental and control caps. A value of $P < 0.05$ was considered statistically significant.

Results

Healing progressed uneventfully, without complications, in all animals. There was no sign of postoperative infection in any of the animals used in the experiment.

The micro-CT images showed the mass of graft material in the experimental site at week 0. The contrast of the mineralized tissue gradually and time-dependently increased in both the experimental and control sites. At 12 weeks, the mineralized tissue reached the top of the plastic cap at the experimental sites; it reached approximately half the height of the plastic cap at the control sites (Figs. 4, 5).

The I-VIEW images illustrated the dynamics of bone

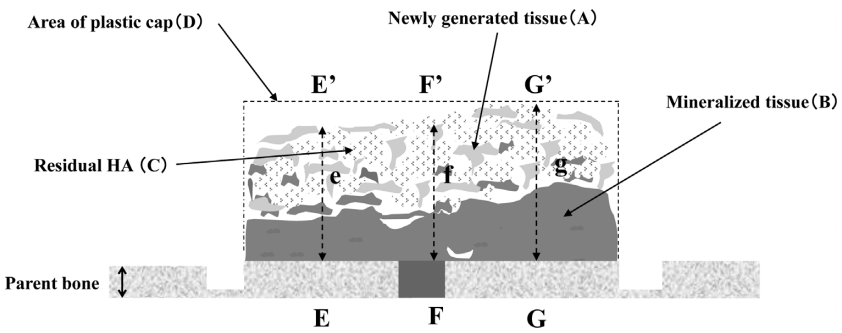

Percent of newly generated tissue A/A+B+C+D × 100

Percent of mineralized tissue B/A+B+C+D × 100

The height of newly generated tissue (Ee/EE'＋Ff/FF'＋Gg/GG')/3 × 100

Fig. 3 The measurements made on histological sections.

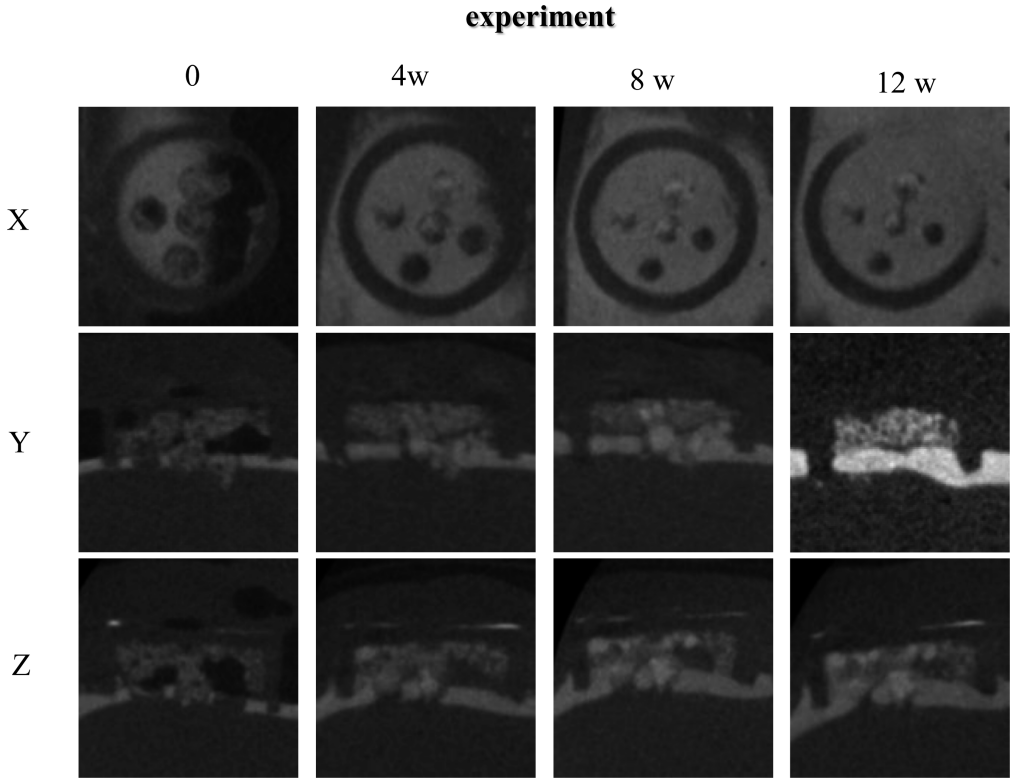

Fig. 4a The x-y-z image of a plastic cap at the experimental site, processed using 3-dimensional imaging software.

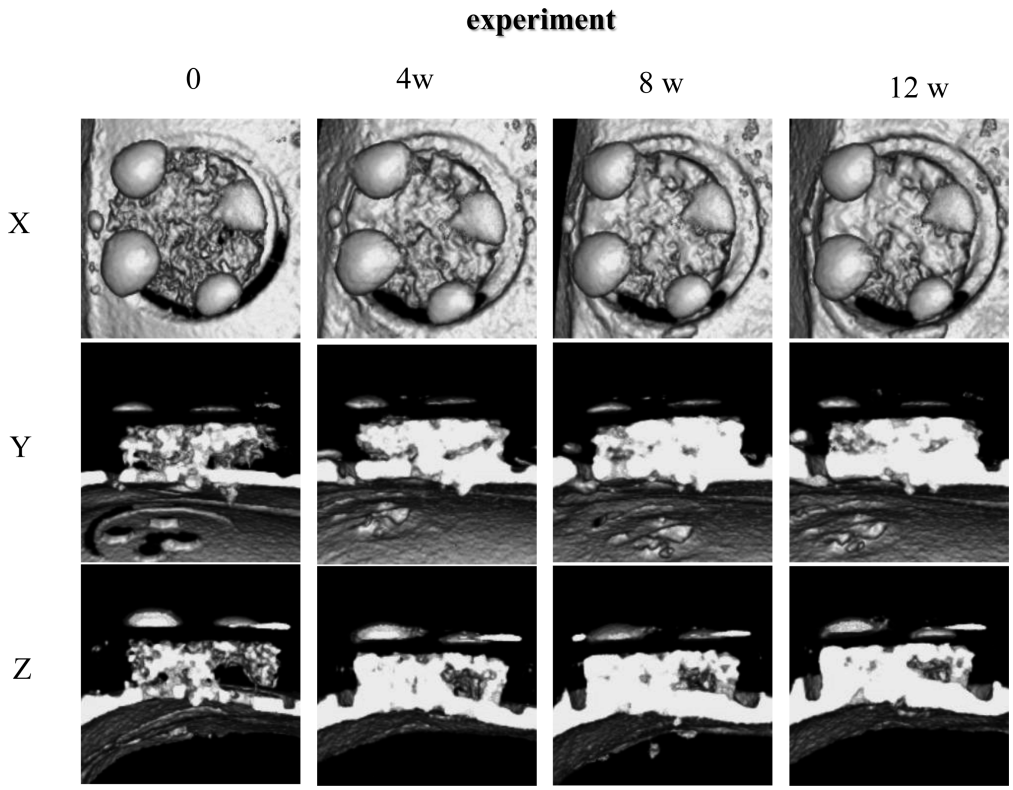

Fig. 4b The x-y-z image of a plastic cap at the experimental site, processed with 3-dimensional imaging software.

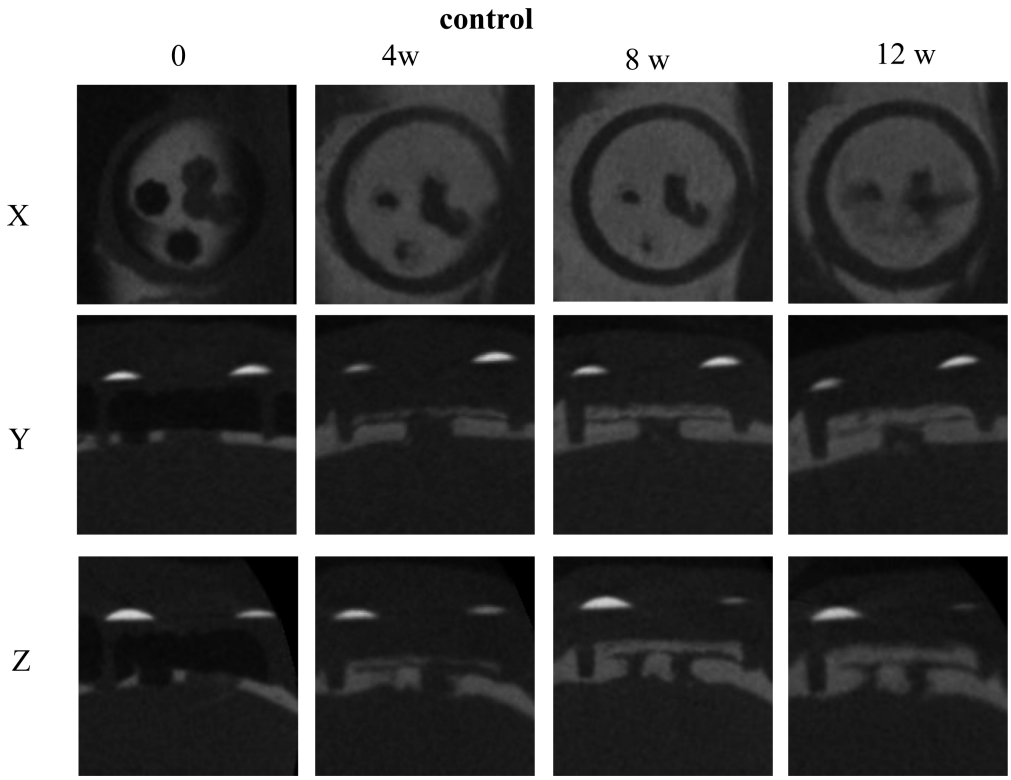

Fig. 5a The x-y-z image of a plastic cap at the control site.

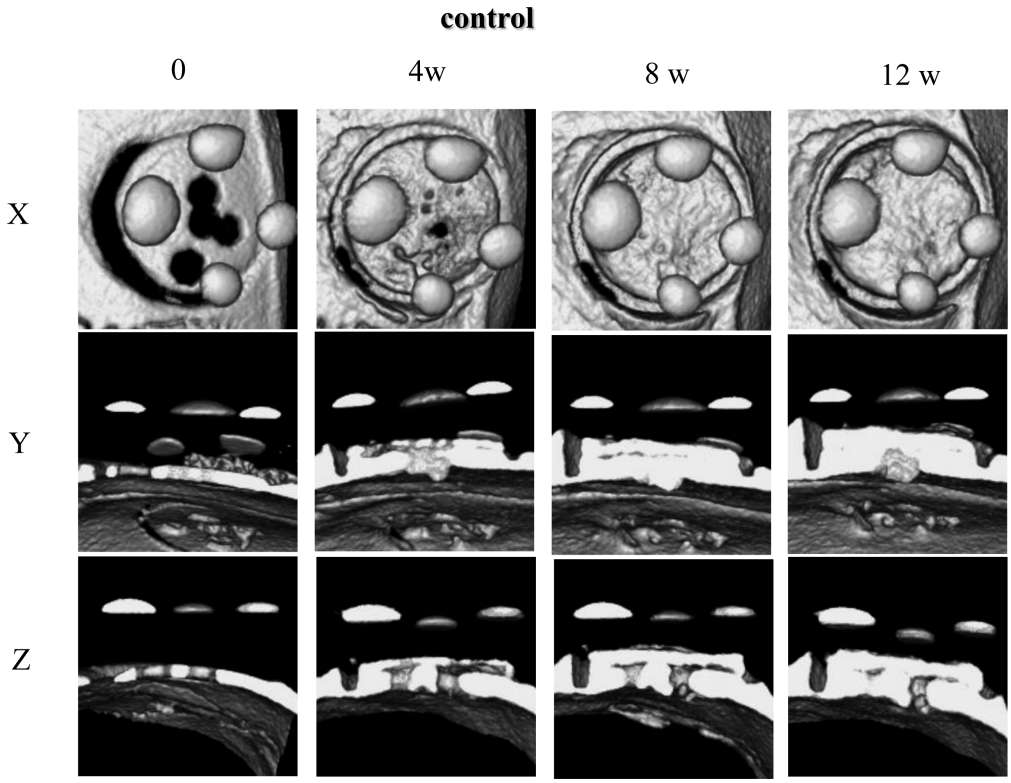

Fig. 5b The x-y-z image of a plastic cap at the control site, processed with 3-dimensional imaging software.

augmentation along the xyz axes. The images showed that the mineralized bone increased and almost reached the top of the plastic cap at 4 weeks in the experimental sites, and that a thin layer of mineralized tissue increased gradually until 8 weeks at the control sites (Fig. 6).

A thin layer of newly generated lamellar bone was

Fig. 6a

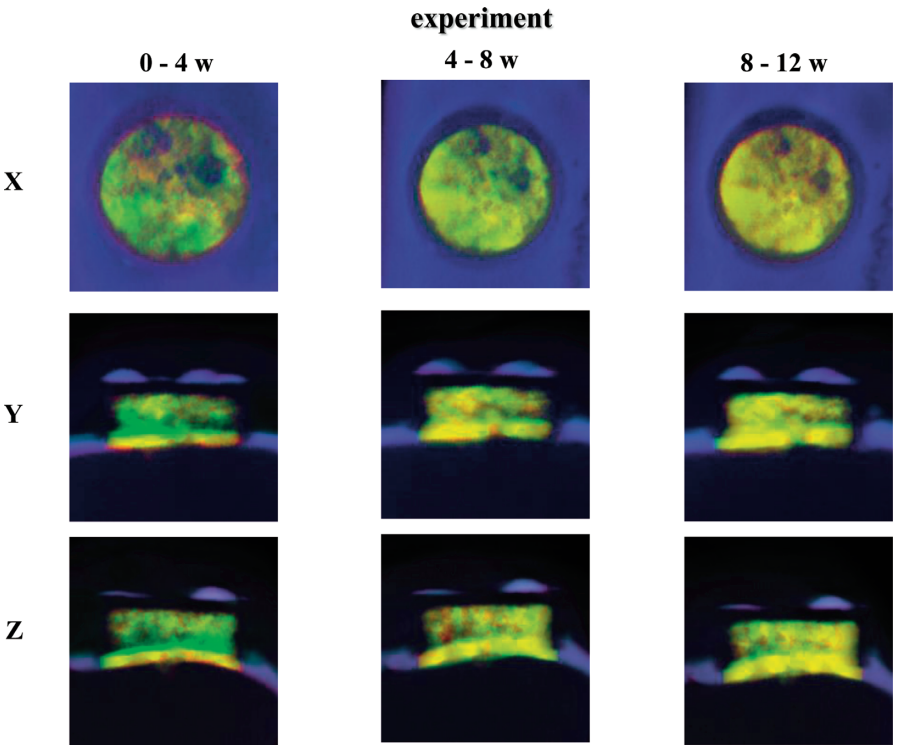

Fig. 6b

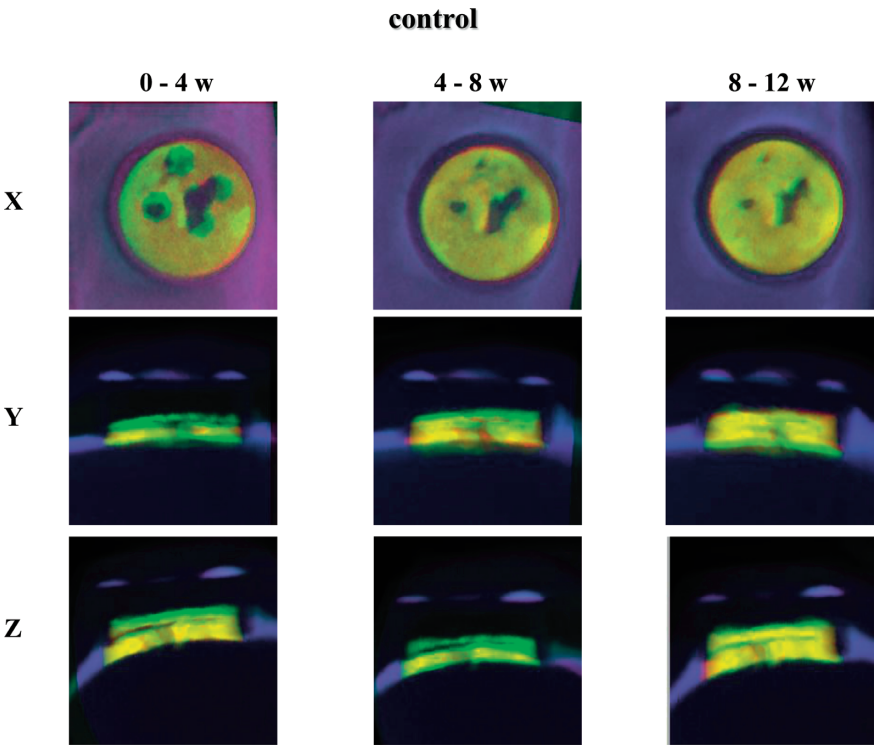

Fig. 6 The x-y-z images of plastic caps at the a) experimental and b) control sites, visualized using I-VIEW software. Green, newly mineralized tissue; red, absorbed bone; yellow, no change.

present on the surface of the parent bone at both the experimental and control sites. Newly generated tissue, a thin layer of mineralized tissue, and residual HA particles were observed over the thin layer of lamellar bone at the experimental site. In addition, the newly generated tissue almost reached the top of the plastic cap at the experimental site; it reached to only half the height of the plastic cap at the control sites.

The histological sections showed a high degree of agreement with the CT images, and consistent patterns of bone formation were observed in both the CT images and histological sections (Fig. 7).

The series of R_mCT images was assessed using subtraction images to distinguish augmented bone under the caps. The data from the morphometric analysis are presented in Figure 8. BV time-dependently increased at both the experimental and control sites. Change in BV did not differ significantly between the experimental and control sites at any experimental time point.

In the histological sections at 12 weeks, the experimental and control sites differed significantly in the total percentages of areas of newly generated tissue and mineralized tissue under the plastic cap; the height of newly generated tissue was significantly greater at the experimental site (Table 1).

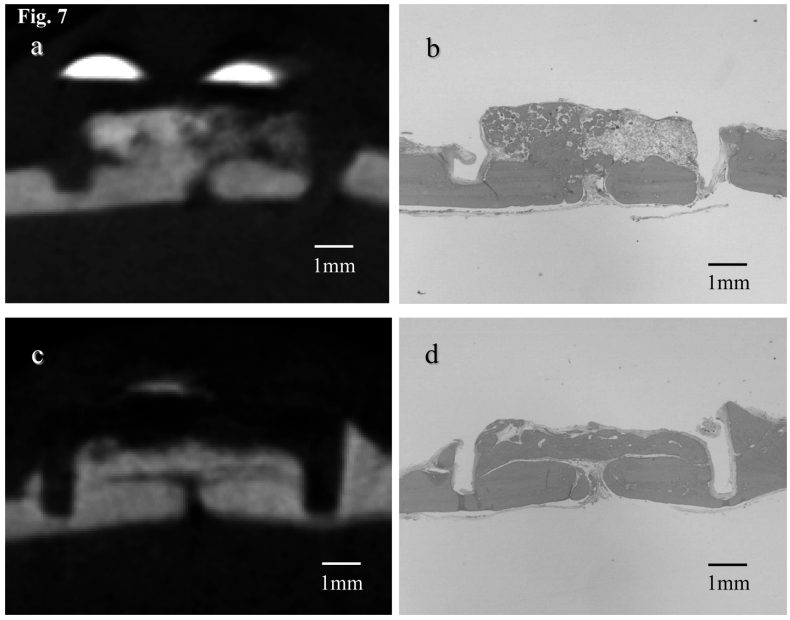

Fig. 7 R_mCT images and histological sections at 12 weeks at the experimental (a, b) and control sites (c, d).

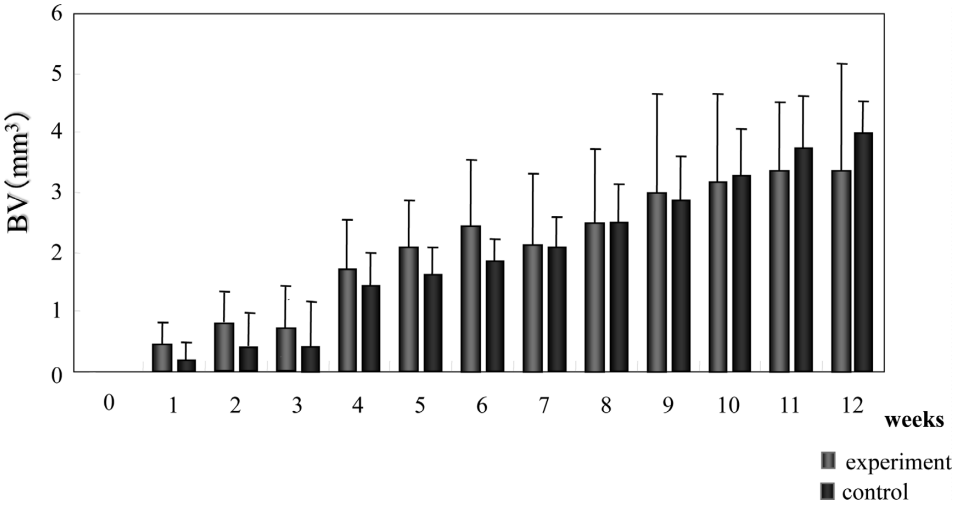

Fig. 8 The bone volume change in the regenerated mineralized tissue within the plastic cap.

Table 1 The amount of newly generated tissue and mineralized bone at 12 weeks

	Newly generated tissue	Mineralized tissue
Experiment	76.3 ± 9.3] *	48.2 ± 10.2] *
Control	38.6 ± 7.6	30.1 ± 10.9
	The height of newly generated tissue	
Experiment	92.6 ± 7.2] *	
Control	36.8 ± 12.5	

$n = 8$, unit = %, * Wilcoxon ranked test, $P < 0.05$

Discussion

This study showed that new bone was generated beyond the skeletal envelope in rat calvaria, with and without HA. Our previous study evaluated the healing pattern of newly generated bone beyond the skeletal envelope in rat calvaria, with and without HA, for up to 12 weeks postoperatively (14). In that study, R_mCT images showed that new bone formed beyond the skeletal envelope at the experimental site, but not at the control site, in rat calvaria. This was due to differences in the experimental model. Critical-size calvaria defects were created in our previous study; however, no bone defects were created in the present study. Because the parent bone can supply a large number of mesenchymal stem cells, total BV in the present study was higher than in our previous study at both the experimental and control sites.

In our previous study, a cylindrical plastic cap was attached with a light-cured composite resin (14). However, the cap sometimes sank into the dural space. Thus, in the present study, we prepared a circular groove and fixed the plastic cap into the groove to prevent this.

Histological analysis is considered the gold standard for evaluating bone growth in bony defects (15). Direct comparison of micro-CT images with histology in rat confirmed good agreement with respect to fine bone detail. Marechal et al. (16) used micro-CT and histological sections to examine the extent of bone augmentation underneath an occlusive membrane; the results were highly correlated. Umoh et al. (17) compared histological assessments and *in vivo* micro-CT images and observed consistent patterns of bone formation in both. Our results also showed a consistent pattern of bone formation on both CT and histological images. The use of micro-CT imaging maximizes the results from each animal, provides sequential data from individual animals, and reduces the required number of animals per study. However, micro-CT does have limitations: it is impossible to evaluate bone growth at the cellular level, and only mineralized tissue can be examined.

The percentage of area of newly generated tissue and the height of newly generated tissue both differed significantly between the experimental and control sites. These results were consistent with our previous rabbit study (10). Bone formation reached the top of the plastic cap within 4 weeks at the experimental sites; at the controls sites, bone increased gradually and reached only half the height of the plastic cap at 8 weeks. This suggests that HA graft material serves as a scaffold, thereby accelerating bone formation.

The total percentage of area of mineralized bone differed significantly between the experimental and control sites in histological sections, although BV did not. This was because assessment of BV change was based on voxels, not pixel images. A further limitation is that the histological sections show only 1 specific area of cross-section, which does not necessarily reflect the entire quantity of augmented bone.

The histological sections showed that a thin layer of lamellar bone was generated over the parent bone at both the experimental and control sites. There was no bone marrow space or trabecular bone structure. In our previous study using a rabbit model of bone augmentation we observed that the newly generated tissue consisted of varying amounts of slender mineralized bone and large marrow spaces (4,10). These disparities might result from interspecies differences in the characteristics of the parietal bone structure. In rat, the parietal bone consists only of lamellar bone; however, in rabbit it has bone marrow and trabecular bone structures. The presence of imprinted topographical information in regenerating tissue might restrict regeneration to restoration of the original morphology (5).

In conclusion, R_mCT analysis allows for highly quantitative and qualitative measurements of mineralized tissue. However, it cannot be used to evaluate the maturation of new tissue or to monitor changes at the cellular level.

References

1. Jensen OT, Greer RO Jr, Johnson L, Kassebaum D (1995) Vertical guided bone-graft augmentation in a new canine mandibular model. Int J Oral Maxillofac Implants 10, 335-344.
2. Lundgren D, Lundgren AK, Sennerby L, Nyman S (1995) Augmentation of intramembraneous bone beyond the skeletal envelope using an occlusive titanium barrier. An experimental study in the rabbit. Clin Oral Implants Res 6, 67-72.
3. Lundgren AK, Lundgren D, Hämmerle CH, Nyman S, Sennerby L (2000) Influence of decortication of the donor bone on guided bone augmentation. An experimental study in the rabbit skull bone. Clin Oral Implants Res 11, 99-106.

4. Min S, Sato S, Murai M, Okuno K, Fujisaki Y, Yamada Y, Ito K (2007) Effects of marrow penetration on bone augmentation within a titanium cap in rabbit calvarium. J Periodontol 78, 1978-1984.
5. Schmid J, Hämmerle CHF, Olah AJ, Lang NP (1994) Membrane permeability is unnecessary for guided generation of new bone. An experimental study in rabbit. Clin Oral Implants Res 5, 125-130.
6. Hämmerle CHF, Karring T (1998) Guided bone regeneration at oral implant sites. Periodontol 2000 17, 151-175.
7. Buser D, Brägger U, Lang NP, Nyman S (1990) Regeneration and enlargement of jaw bone using guided tissue regeneration. Clin Oral Implants Res 1, 22-32.
8. Buser D, Dula K, Hess D, Hirt HP, Belser UC (1999) Localized ridge augmentation with autografts and barrier membranes. Periodontol 2000 19, 151-163.
9. Schmid J, Hammerle CH, Fluckiger L, Winkler JR, Olah AJ, Gogolewski S, Lang NP (1997) Blood-filled spaces with and without filler materials in guided bone regeneration. A comparative experimental study in the rabbit using bioresorbable membranes. Clin Oral Implants Res 8, 75-81.
10. Murai M, Sato S, Fukase Y, Yamada Y, Komiyama K, Ito K (2006) Effects of different sizes of β-tricalcium phosphate particles on bone augmentation within a titanium cap in rabbit calvarium. Dent Mater J 25, 87-96.
11. Benqué E, Zahedi S, Brocard D, Marin P, Brunel G, Elharar F (1999) Tomodensitometric and histologic evaluation of the combined use of a collagen membrane and a hydroxyapatite spacer for guided bone regeneration: a clinical report. Int J Oral Maxillofac Implants 14, 258-264.
12. Arai Y, Yamada A, Ninoyama T, Kato T, Masuda Y (2005) Micro-computed tomography newly developed for in vivo small animal imaging. Oral Radiology 21, 14-18.
13. Min S, Sato S, Saito M, Ebihara H, Arai Y, Ito K (2008) Micro-computerized tomography analysis: dynamics of bone augmentation within a titanium cap in rabbit calvarium. Oral Surg Oral Med Oral Pathol Oral Radiol Endod 106, 892-895.
14. Kochi G, Sato S, Fukuyama T, Morita C, Honda K, Arai Y, Ito K (2009) Analysis on the guided bone augmentation in the rat calvarium using a microfocus computerized tomography analysis. Oral Surg Oral Med Oral Pathol Oral Radiol Endod 107, e42-e48.
15. Cowan CM, Aghaloo T, Chou YF, Walder B, Zhang X, Soo C, Ting K, Wu B (2007) MicroCT evaluation of three-dimensional mineralization in response to BMP-2 doses in vitro and in critical sized rat calvarial defects. Tissue Eng 13, 501-512.
16. Marechal M, Luyten F, Nijs J, Postnov A, Schepers E, van Steenberghe D (2005) Histomorphometry and micro-computed tomography of bone augmentation under a titanium membrane. Clin Oral Implants Res 16, 708-714.
17. Umoh JU, Sampaio AV, Welch I, Pitelka V, Goldberg HA, Underhill TM, Holdsworth DW (2009) In vivo micro-CT analysis of bone remodeling in a rat calvarial defect model. Phys Med Biol 54, 2147-2161.